CFD investigations of venting systems for pollutant dispersion

Kashef, A.; Baskaran, B. A.; Anantaraman, A.

CFD INVESTIGATIONS OF VENTING SYSTEMS FOR POLLUTANT DISPERSION

Drs. A. Kashef and A. Baskaran
Institute for Research in Construction
National Research Council Canada
Ottawa, Ontario, Canada K1A 0R6

Dr. A. Anantaraman
Electrochemical Science and Technology Center
University of Ottawa
Ottawa, Ontario, K1N 6N5

ABSTRACT

To investigate the ventilation rate of hydrogen gas in battery pockets, IRC used the Computational Fluid Dynamics (CFD) tools and techniques. IRC formulated a numerical model using, the 3D Navier Stokes Equations (NSE) together with the standard k -- ε turbulence model. For the model development, the control volume technique is employed to discretize the differential equations into difference form and the developed model has been used to simulate the ventilating process of the hydrogen gas. The paper presents and discusses the numerically computed results for nine different venting configurations. A ranking criteria has been developed to offer an optimum design condition based on computed results for the nine studied configurations. Recommendations are made based on the system efficiency in ventilating the hydrogen gas.

INTRODUCTION

Environmental scientists have applied experimental procedures to predict the dispersion of air born pollutants such as hydrogen gas propagation. Thorough understanding of air flow behavior can significantly help in identifying gas pollution dispersion process. This knowledge is usually obtained through laboratory experiments and field measurements. Alternatively, advancement in Computational Fluid Dynamics (CFD) offers a new non-hazardous method of analysis to understand, visualize and quantify flow field distribution and hence gas dispersions. Interested readers in the latest applications of CFD are referred to Baskaran and Stathopoulos (1994).

Hydrogen gas production was observed from a facility that stores bank of lead-acid. Venting arrangements exist, as shown in figure 1, to prevent the hydrogen gas build up inside the facility.

The venting arrangement consists of two venting tubes each of 25.4 mm (1") diameter. The left tube is 1500 mm length projecting outside the battery pocket. Total length of the right tube is 3200 mm. Of this length, 1700 mm is inside the battery pocket and 1500 mm projects outside the battery pocket. Both the two venting tubes have bents at the top of 146 mm length. However, it has been reported that the level of hydrogen gas concentration inside the battery pocket is not acceptable and might cause hazard problems. Therefore, further investigations are performed, using this venting system as the base configuration, to evaluate the efficiency of different venting arrangements. For this purpose, the hydrogen gas movements inside the buoy battery pockets have been simulated and its ventilation rate has been computed using CFD technique.

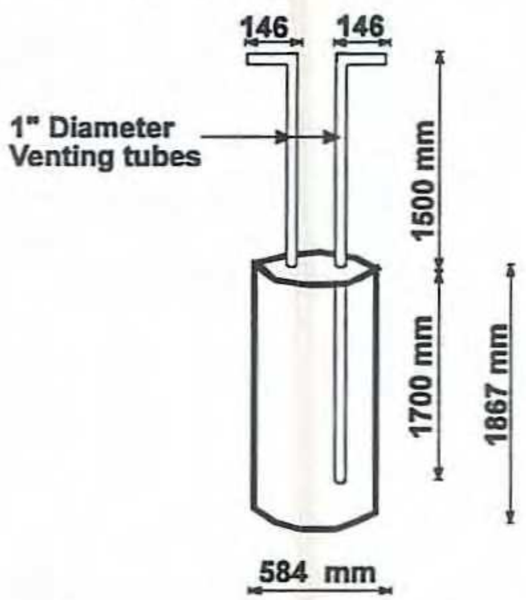

Figure 1 Existing Venting Arrangements

Based on the above discussion, the main objectives of the present investigation are

(1) Produce decay rate curves of hydrogen gas for the various modeled configurations.
(2) Examine the effect of different venting systems on hydrogen gas decay rate.

MODELED CONFIGURATIONS

To undertake the numerical investigations, the venting system shown in Figure 1 has been modified and modeled. The hydrogen production is simulated by injecting the hydrogen gas at a rate of 12 ml/min through a side opening at a height of 900 mm. Figures 2 and 3 show all the modeled configurations. Modeled configurations are divided in to two main groups. Group 1 tube venting arrangement and Group 2 hole venting arrangements. Under the first group, the hydrogen gas is mainly ventilated through two tubes each of 25.4 mm (1") diameter, Figure 2. The left tube is 1500 mm length projecting outside the battery pocket. The right tube has various dimensions. For Configurations 1, 2, 3 and 5, the right venting tube is of total length 3200 mm. Of this length, 1700 mm is inside the battery and 1500 mm projects outside the battery. For configuration 4, the right tube only extends outside the battery pocket and has a length of 1500 mm. Both the two venting tubes have bents at the top end except for Configuration 2.

Figure 3 presents the second venting arrangement, namely, hole venting group. Under this group the hydrogen gas is mainly ventilated through two holes at the top of the battery pocket placed at equal distances from the center of the battery pocket. The size of the venting holes varies from 5 mm (≈ 2") to 8 mm (≈ 3") in diameter. Configuration 7 has the two holes covered with a special porous material. The material has a 50 % porosity to gas while it has 0 % porosity for water. Configuration 9 is performed to study the volume effect on hydrogen ventilation. It is identical to Configuration 8 but the volume of the battery pocket is half as much. The diameter of the two holes is kept equal to 8 mm (≈ 3").

Method of Analysis

The present analyses were conducted using, the well-known commercial CFD solver, PHOENICS (Spalding, 1981) (Parabolic Hyperbolic Or Elliptic Numerical Integration Code Series) version 2.0. This has been achieved by preparing an appropriate input file (Q1 file) as described in the CHAM (1989), PHOENICS reference manual. For the present study, solved variables are: pressure p; velocity components, u, v and w in the cylindrical directions, x (tangential), y (radial), and z (vertical) respectively; concentration of hydrogen gas; and kinetic energy, k; its dissipation rate, ε. PHOENICS provides solutions to the discretized versions of sets of differential equations of the following general form:

$$\frac{\partial(r\rho\varphi)}{\partial t} + div(r\rho\varphi v - r\Gamma\phi grad\phi) = rS \qquad (1)$$

transient convection diffusion source

where: t is the time; r is the volume fraction; ρ is the density; ϕ is the dependent variable; v is the velocity vector; Γ_ϕ is exchange coefficient of entity ϕ; and S is the source rate of ϕ

A 3D grid system is developed for each configuration. For the problem at hand, it was found that using a system of cylindrical axes is most appropriate. In this system of axes, x-axis represents the tangential direction; the y-axis is the radial distances and the z-axis is the vertical distances. A typical 3D grid system for Configuration 1 is shown in Figure 4. Grids are denser at the inlet where injection of hydrogen gas takes place. The domain consists of 32 x 20 x 52 nodes along x, y, and z directions respectively.

These computations are repeated 48 times. The 48 time steps correspond to 24 hours of hydrogen gas ventilation observations with 1/2 hour as time increments. At each time step the computations are repeated for several numbers of iterations. At the end of the iterations, the normalized error is computed to be 0.1. The number of iterations is selected after carrying out sensitivity studies as described by Baskaran (1990).

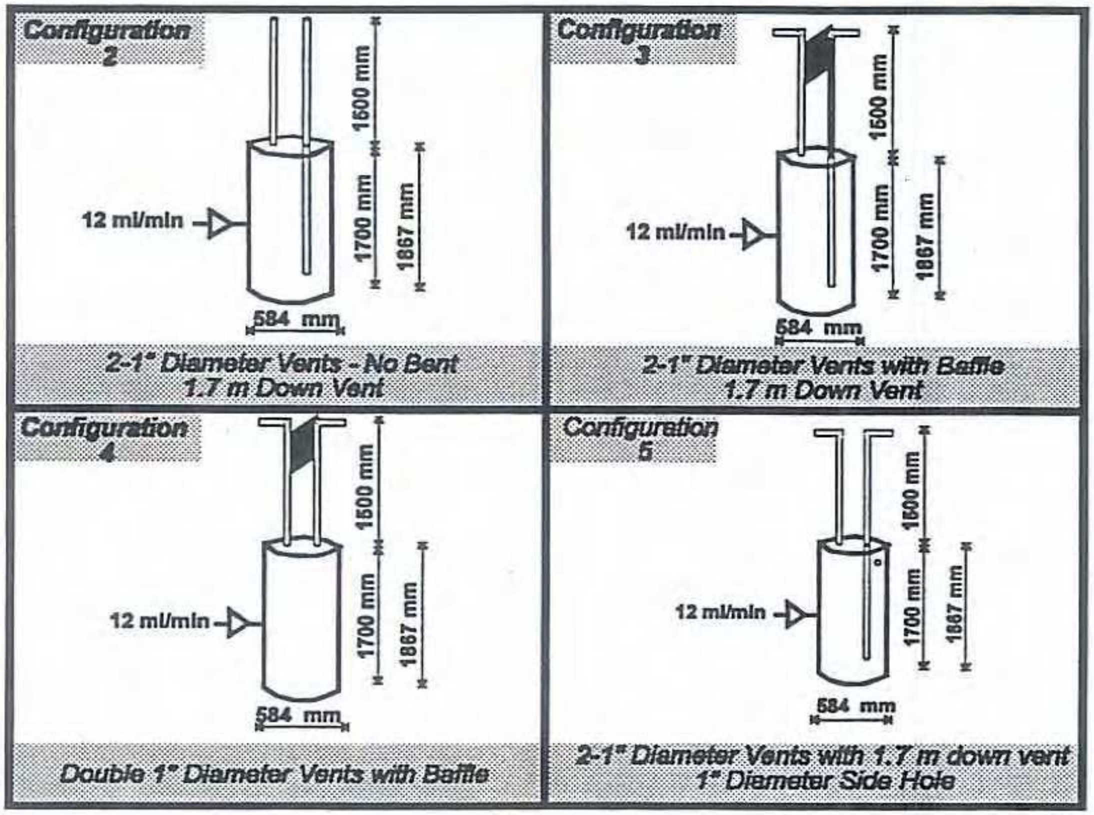

Figure 2 Tube Venting Arrangements – Group 1

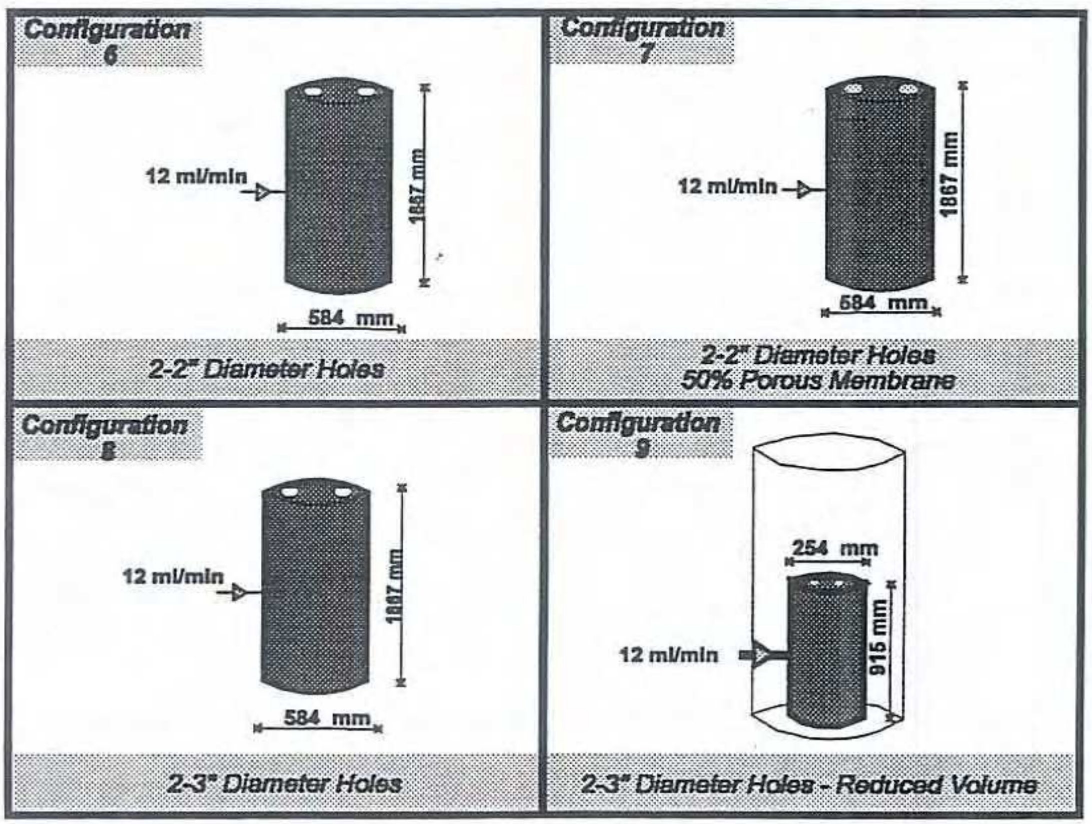

Figure 3 Hole Venting Arrangements – Group 2

RESULTS AND DISCUSSION

Results obtained from the investigation of the nine configurations were visualized using FAST. FAST (Flow Analysis Software Tool kit) is a software environment for data visualization (Walatka, 1992) animation package. A special transfer protocol has been developed to transfer the data from PHOENICS to FAST and recorded in video cassettes. This facilitated the visualization of hydrogen ventilation process.

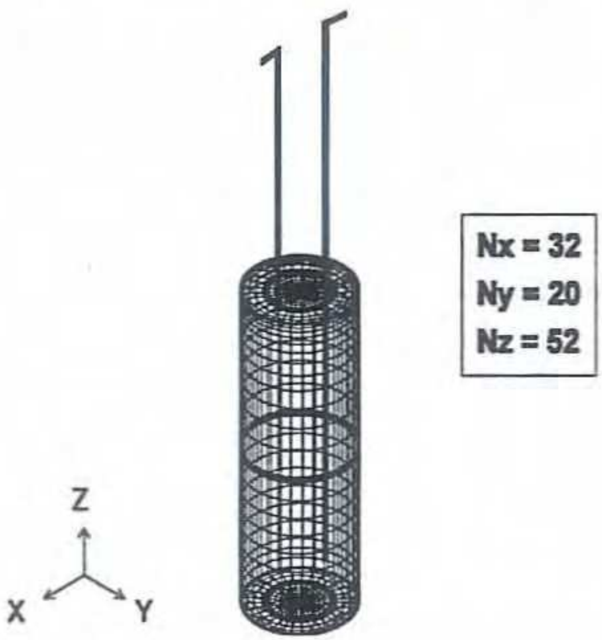

Figure 4 Grid System for Base Configuration

One such converted plot is shown in Figure 5, representing for the Configuration 1 at time step 16 hours. In that plot, the vectors are distinguished with their length, instead of color for this particular presentation. Longer arrows represent higher values of flow velocities and shorter vectors are indication of low values of flow velocities. It is clear from the figure that due to the turbulent areas at the bend change in direction and reduction in flow velocities are taking place at these areas. Moreover, reversed flow areas are observed in the two venting tubes causing reverse venting process. Comparison of configuration 2 with Configuration 1 (see figure 2), the reversed flow phenomenon associated with the presence of bends can be eliminated. Similar visualizations were made to compare the overall performance of the modeled configurations.

The results of CFD analysis are further compiled into decay curves of hydrogen concentration. In the development of such curves, the concentration of hydrogen gas L.E.L percentage units are plotted against time for several critical spots inside the battery pocket for each modeled configuration to determine inclusively the performance of each ventilation arrangement. Figure 6 shows the decay curves of hydrogen concentration in for Configuration 1. The vertical axis is the hydrogen concentration values L.E.L percentage units. The horizontal axis is the time axis ranging from 0 to 24 hours. At each selected location, a decay curve based on collection of 48 data sets is plotted. As observed from the Figure, these curves are distinct for different locations. The range of discrepancy is quite large as indicated in Figure 5. To inclusively predict the performance of this ventilation arrangement, an envelope decay curve is drawn, dashed line, to embody all these decay curves. Thus to determine the maximum concentration of hydrogen gas in the battery pocket at any given time, one can enter the curve at the required time to obtain the corresponding maximum hydrogen concentration in L.E.L% from the envelope curve.

Figure 7 shows a comparison between the experimental and numerical data for the base configuration. The comparison is done for the results at an observation point 800 mm from the top. The experimental data is collected at a similar location. It is clear from the figure that trend of decay curve is successfully reproduced by the numerical analysis. Some of the difference of values between the experimental and numerical data is attributed to the fact that the experiment in this case started at a non-zero value of hydrogen concentration. The insufficient number of experimental data (four data sets) also contributes to the discrepancy.

Group 1 – Tube Venting Arrangements

Figure 8 shows the performance curves for all computed Group 1 cases. These curves are obtained as explained following a similar procedure used for figure 6. There are four curves representing four modeled configuration with tube venting arrangements. For comparison purpose, the curve representing the

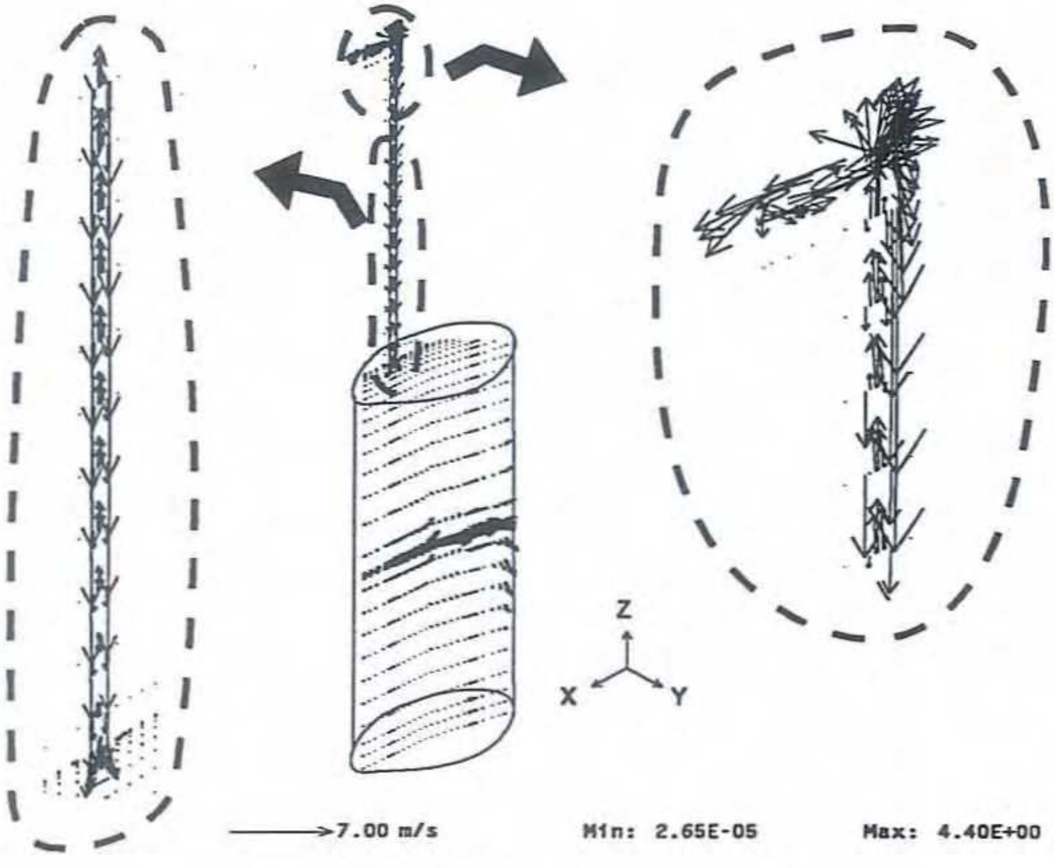

Figure 5 Flow Movement - Base Configuration

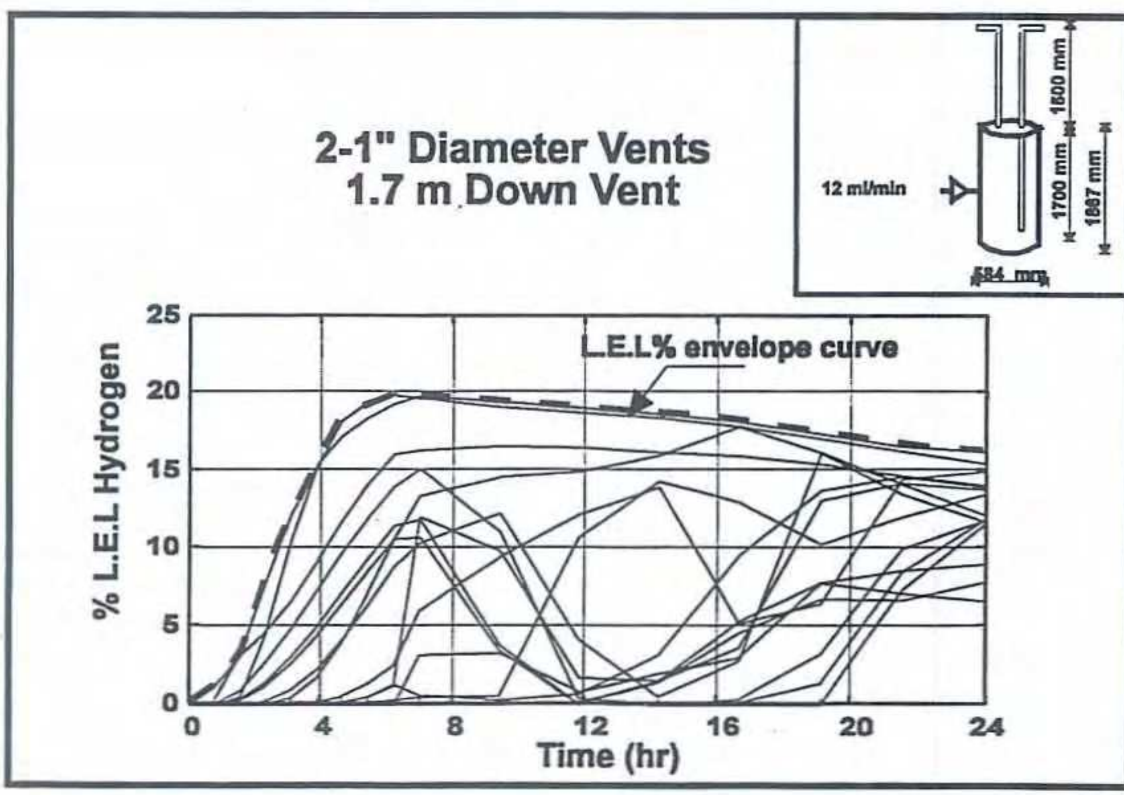

Figure 6 Development of an Envelope Decay Curve – Base Configuration

base configuration is also included. All curves show build up for the first 8 hours and the decay process starts after that and continues till the end. The baffle configuration has the highest build up whereas the base configuration has the minimum decay. The configuration representing with 1" holes on the sides has the minimum build up (about 18 % of LEL) and maximum decay (about 13% of LEL) for this group.

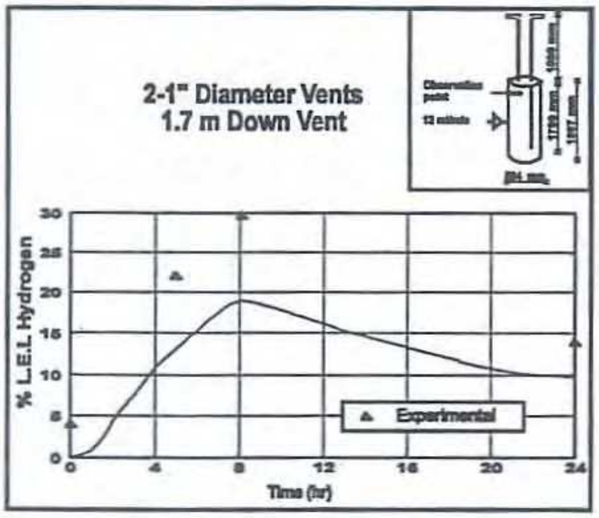

Figure 7 Comparison between Experimental and Numerical Results – Base Configuration

Group 2 — Hole Venting Arrangement

The envelope decay curves for configurations 6 through 9 are drawn in Figure 9. The construction of these envelope curves is identical to that used to plot Figure 6. As explained before, all curves follow the build up and decay process. However, only for configuration 9, the build up continues up to 8 hour period. For remaining configuration (6,7 and 8), the build up reaches maximum at 4 hours and the system maintains constant LEL level up to 8 hours. After 8 hours the decay process starts. This indicated that these three configurations ventilating even during the injection period. The merits of these envelope decay curves will be discussed in later sections.

RANKING ANALYSIS

It is necessary to formulate a criterion by which one can rank the different modeled configurations with view to their ventilation performance.

The decay curve, as viewed in Figure 10, can be divided into two main regions; namely, build up region and decay region. The build up region extends over the injection period of hydrogen (eight hours). On the other hand, the decay region continues over the remaining duration of 16 hours. Accordingly, two criteria are adopted in the ranking procedure to reflect such regions. The first criterion, related to the build up region, is called ***preventive measure*** which is a measure of venting efficiency during injection of hydrogen and is measured by η_b. To measure the venting efficiency after the termination of hydrogen injection, the ***remedial measure*** criterion is adopted which can be measured by η_d. The two venting efficiencies can be respectively calculated from:

$$\eta_b = \left[1 - \frac{\text{Peak value}}{\text{Maximum peak}}\right] * 100\% \quad (2)$$

$$\eta_d = \left[1 - \frac{\text{Decay value}}{\text{Maximum peak}}\right] * 100\% \quad (3)$$

In Equation 2 and 3, the different terms are defined as follows, Figure 10: η_b is the injection venting efficiency; η_d is the decay venting efficiency; *peak value* is the hydrogen concentration value at the end of 8 hours for a particular configuration; decay value is the hydrogen concentration value at the end of 24 hours for a certain configuration; and *maximum peak* is the maximum concentration value at the end of 8 hours among the nine modeled configurations. In ranking the different venting systems, the following considerations are taken into account:

- The higher the values of the efficiencies η_b and η_d, the better the venting arrangement performance is.
- Higher η_b indicates a simultaneous ventilation process during the input of hydrogen and lower build-up of hydrogen concentration is expected during the decay. Thus, priority in ranking is given for higher η_b.

The values needed for the ranking analysis are extracted from the computed data for all nine configurations and they are presented in Table

1. For a comprehensive evaluation of the venting system performances, the values reported in Table 1 are those for the envelope decay curves (Figure 8 and 9). Table 1 displays the calculated efficiencies for the nine modeled configurations. Based on the above-mentioned considerations, the ranking is performed and presented in Table 1.

Table 1 indicates Configuration 8 to have the best ventilation performance. On the other hand, Configuration 9 is considered the worst with regard its ventilation performance. Also, the base configuration (Configuration 1) stands in the middle of the ranked configurations.

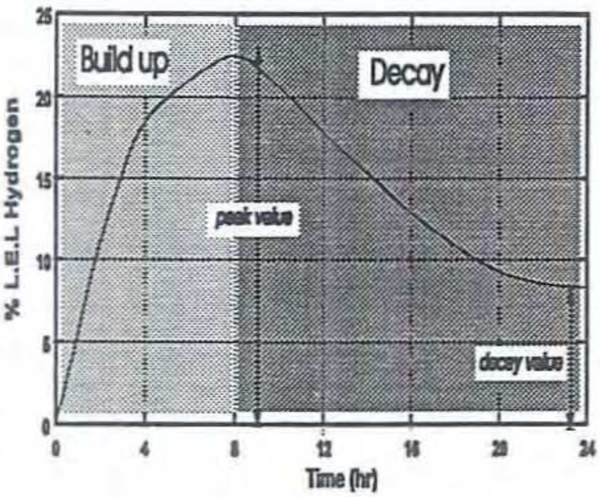

Figure 10 Two Regions of a Decay Curve

Configuration No.	Rank	η_b	η_d
8	1	31	41
6	2	30	40
2	3	18	34
5	4	17	40
1	5	14	28
7	6	14	28
3	7	12	37
4	8	10	34
9	9	0	39

Table 1 Ranking of Modeled Configurations

SUMMARY

A systematic numerical investigation is undertaken at IRC for the prediction of hydrogen gas ventilation process in buoy battery pockets. CFD technique is used for this analysis. Due to its inherent advantage, CFD modeling offers extensive insight on hydrogen gas propagation inside the battery pocket. The results of these analyses are further used to perform a ranking analysis among the studied configurations.

Among the first group of venting arrangements, using tubes as venting, Configuration 2 is presumed to have the best ventilation performance. In the other group, holes as venting, the 3" diameter hole offered better venting performance

REFERENCES

1 A. Baskaran, "Computer Simulation of 3D Turbulent Wind Effects on Buildings", Ph.D. Thesis, Concordia University, Montreal, Canada, 1990.

2 A. Baskaran and A.H. Kashef, "Investigation of Air Flow around Buildings Using Computational Fluid Dynamics Techniques," Paper accepted for publication in the Special Issue of Engineering Structures Devoted to Computational Wind Engineering, January 1996.

3 CHAM Development Team, The PHEONICS - 1.6.6 User Guide, CHAM, Bakery House, 40 High Street, Wimbledon, London SW19 5AU, UK, 1989.

4 D.B. Spalding, "A General Purpose Computer Program for Multi-dimensional One and Two-phase Flow", Math and Comp. Simulation, XXIII, 267, 1981.

5 P. Walatka, FAST Maps- User Interface- FAST Beta 2.1, NASA Ames Research Center: WAO and RND, April 1992.

6 A. Ronold, "Modeling of Flow and Ventilation within Petroleum process Plants", First International Symposium on Computational Wind Engineering, Tokyo, pp 54-59, 1992.

7 S. V. Patankar, "Numerical Heat Transfer and Fluid Flow", Hemisphere Publishing Corporation, McGraw-Hill Book Company, 1980.